COMADEM 2011
Proceedings of the 24th INTERNATIONAL CONGRESS on
Condition Monitoring and Diagnostics Engineering Management
Clarion Hotel Stavanger, Stavanger, Norway, 30th May – 1st June, 2011
(Editors) Maneesh Singh, Raj B. K. N. Rao and J. P. Liyanage,
COMADEM International, U.K., ISBN: 0-9541307-2-3

Performance characteristics of a Vertical Axis Wind Turbine (VAWT) under transient conditions

Gareth Colley[1], Dr. Rakesh Mishra[2], Prof Vasu Rao[3],

Department of Engineering & Technology, Univesity of Huddersfield, Queensgate, Huddersfield, HD1 3DH.
g.colley@hud.ac.uk/r.mishra@hud.ac.uk

ABSTRACT

The present work investigates the performance characteristics of a novel Vertical Axis Wind Turbine (VAWT) for use in the urban environment. Here the performance of the wind turbine has been analyzed experimentally using a full scale prototype measuring 2.0m diameter and 1.0m in height. The turbine was located at the exit of a 0.6m x 0.6m wind tunnel section and was subjected to a jet flow. The performance output from the turbine has been obtained using a torque transducer unit which provides instantaneous torque and speed data. This data has been used to validate a computational model generated from Computational Fluid Dynamics (CFD) software code Fluent where a Multi Reference Frame (MRF) approach has been used. It is shown that the MRF solving technique under predicts rotor torque at high rotor speed and does not predict rotor suction effects on an upstream stream wise velocity profile. It is concluded that such variations between experimental and computational velocity fields is the primary factor that effects rotor torque output.

Keywords : Vertical axis, Turbine, Performance, Torque, CFD, MRF

1. INTRODUCTION

Renewable energy technologies play a key role in the contribution to sustainable energy as a whole. Such technologies reduce our dependency on fossil fuel reserves and pave the way for long term energy security. Wind power falls into this category and has been harnessed for hundreds of years to perform mechanical work and generate power. . From a UK perspective the mainland has limited coal and gas resources but is subjected to high wind speeds. It therefore seems that a strong case for the use of wind power could be argued. With this in mind, wind power is the first renewable power generation technology (excluding large hydro projects) to become a genuine mainstream alternative for increasing the generation capacity across the globe **[1,2]**.

Since the last major European wind energy review in 2004 this sector has seen a rise of 22,000 MW in installed generation capacity by the end of 2007 in Europe alone. This rise has contributed to an increase in global annual growth rates with 60% of installed capacity now present in Europe. This has placed Europe firmly as a global leader in wind energy conversion **[3]**.

In 2008, the world installed in excess of 20,000 MW of wind turbines bringing the world installed capacity over the 100,000 MW milestone. The Global Wind Energy Council (GWEC) has predicted that by 2012 the global installed capacity from wind energy conversion could be as high as 240,000 MW **[3,4]**.

Over the last 30 years significant developments have been made in the wind power sector in the form of design optimization for increased power output. Such developments have been limited in the sense that the basic design principles of the machines limits the scope of design changes that can be carried out. The majority of this design optimization was carried out in the late 70's and early 80's with Sandia Laboratories conducted a vast amount of research. The vertical axis machines namely Savonius and Darrieus have been investigated extensively in the past and the limitations of each design are well documented. The turbine presented in the current work shares many similarities to the Savonius rotor which is shown to generate an opposing torque from the flow interaction with the upwind convex blade. This interaction effect results in opposing torque acting against the direction of motion which is often found on the leeward side of cross flow machines. This effect significantly reduces the peak power output and although this is a fundamental problem little research has been conducted to remove this effect.

Many of the recent developments in turbine design are in the form of novel types of machine particularly those that feature multi blade radial design similar to the turbine in the present work. Takao et al **[5]**

presents a novel radial cross flow wind turbine featuring five equally spaced NACA 0015 profile blades. Surrounding the blade inlet zone is a set of outer guide vanes which are directed into the steam wise flow by a downstream tail vane. The turbine measures 0.6m in diameter and 0.7m in height with the machines performance output determined from wind tunnel tests. Here, the effect of Reynolds number on turbine performance with and without guide vane arrangement has been quantified. The authors report increases in power output of 1.5 times for the turbine with guide vane row. Further investigation have been carried out into the effects if varying rotor solidity in which the number of blades is varied from 2-5. The turbine generates a power coefficient of 0.085 at a tip speed ratio of 0.95 for a five bladed rotor whereas reducing the number of blades results in a power coefficient of 0.15 at a tip speed ratio of 1.6. This highlights both the effect of solidity on peak power but also the speed up effects by reducing the number of blades.

Further novel designs have been documented in the form of utility scale vertical axis turbines. Park and Lee et al **[6,7]** have presented a radial cross flow multi blade VAWT which features a set of outer guide vanes again directed by a downstream tail vane. Here the outer guide vanes are placed upstream and are used to accelerate the flow into the rotor blade passages. A secondary side collector is used to funnel the flow into the passages on the leeward side of the machine which would be otherwise un used. Such modifications have allowed the authors to maximize power output and have reported power coefficients in the order of 0.45 for the baseline six bladed designs. The effects of blade number and turbine aspect ratio on power output have also been quantified with the aim of optimizing power coefficient. It is seen that increasing the blade number from 6 – 9 results in significant increases in power with increases in the order of 13%. Further increases are seen for a blade number of 12 where a 19.5% increase is seen compared to the baseline. It is also seen that the overall power output of the machine is extremely sensitive to aspect ratio and although some data is provided further studies should be carried out.

Such examples of increasing power output are now common place although many of the works focus on the global performance parameters without consideration to the local flow. The present work will investigate the performance characteristics of a novel multi-blade machine using CFD which will be validated against full scale experimental data. The wind turbine presented has similarities to that presented by Park and Lee et al and features an outer set of guide vanes to increase energy capture.

2. EXPERIMENTAL TEST SETUP

The following section describes the experimental test setup used for the validation of CFD data. The validation strategy is in the form of a comparative analysis between experimental and computational data at identical operating conditions.

2.1 Wind Turbine Test Rig

The validation carried out in this study compares a set of experimental data with data obtained from computational analysis. Experimental data is obtained from wind tunnel tests using a full scale prototype turbine. This prototype turbine has been tested at the fluid dynamic laboratory within the University of Huddersfield and measures 2.0m in diameter and 1.0m in height.

The experimental test setup used for this validation consists of a low speed wind tunnel which uses a varofoil single stage axial fan to provide mass flow of air through the test chamber. The wind tunnel is of open circuit type where air is discharged into the laboratory environment. The horizontal axis varofoil fan is controlled via a pneumatic control valve. The valve bleeds off system pressure and is used to control flow speed. Upstream of the test chamber are a set of four manually controlled guide vanes used to condition the flow in the vertical direction. These vanes are position so that their longitudinal axis is parallel to the stream wise flow direction. Due to the rotational characteristics of the flow exiting the fan section a flow straightening section is installed downstream of the guide vanes. This section is in the form of aluminum honeycomb sheet which a cell size of 9mm and sheet thickness of 60mm. The sheet measures 600mm x 600mm in size and is installed directly into the test section inlet. The test chamber consists of four Perspex sheets which have been bonded together to create an air tight 600mm x 600mm square section with a length of the 1.5m. The approximate flow speed range within the chamber is 7m/s to 24 m/s.

The experimental performance tests have been carried out at a constant free-stream velocity of 14.8m/s which is measured within the test chamber. The velocity profile at the exit of the test section has been meaured using a 4 hole coba head pressure probe. It is seen to be non uniform in the ZY plane as per figure 1. The profile is shown below in terms of 49 point velocity values which correspond to the

streamwise flow component only. This is taken to be a one-dimensional flow due to the dominance of the this flow component.

Z COORDINATE POSITION (mm) \ Y COORDINATE POSITION (mm)	0	12	100	200	300	400	500	588	600
0	0	0	0	0	0	0	0	0	0
1.5	0	6.93	8.72	8.56	8.29	9.02	8.45	6.83	0
100	0	8.79	12.1	11.9	11.9	12.6	11.7	9.06	0
200	0	10.5	12.9	12.5	11.9	12	11.2	10.1	0
300	0	9.82	11.2	11.2	10.4	11.5	11.9	10.8	0
400	0	9.73	11	12.2	12.4	12.7	12.9	10.9	0
500	0	8.74	11.1	12.1	11.7	11.5	11.8	9.11	0
598.5	0	6.56	7.98	9.24	8.62	8.41	8.23	6.6	0
600	0	0	0	0	0	0	0	0	0

FIGURE 1. Velocity field at exit of test chamber

The wind turbine is positioned downstream of the test section such that it is not enclosed by any boundaries. The turbines location relative to the test section exit plane is shown in figure 2. Here, the turbines location is dimensionally constrained within the X, Y and Z axis as per the coordinate system described in the figure. The offset distance from the test chamber exit plane in the X axis is defined as 'd' and is 0.5m. The secondary location parameter is 'd1' and acts in the Z axis, this dimension is 0.193m**.** The final constraint is in the Y axis which is not provided on the figure. This constraint requires the outer diameter of the turbine to be tangential to the test chamber wall.

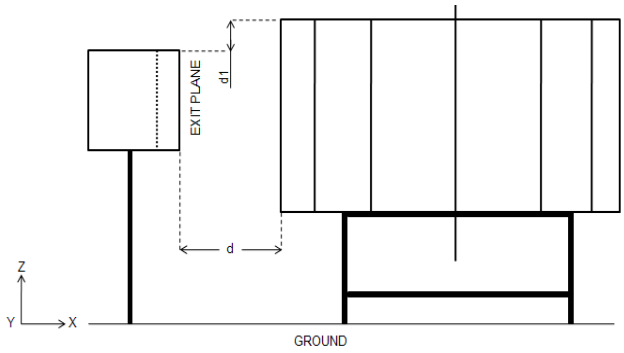

FIGURE 2. Wind turbine location

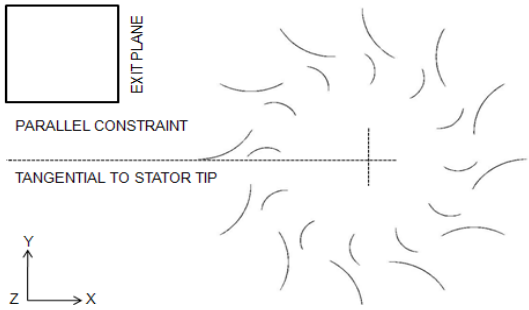

FIGURE 3. Wind turbine geometry positional constraints

As the turbine is circular the location is still under-defined and hence a relation between the turbine blade geometry and test chamber walls has been provied in figure 3. Here the turbine geometry is alligned to the test chamber wall using a parallel constraint between the outer chamber wall and a line that is fixed tangentially to the outer stator tip. This line is taken from the central axis of the turbine geometry and extended radially where it meets the stator tip face.

2.2 Wind Turbine Setup

The wind turbine test setup consists of a torque transducer, driving gear, pinion gear and permanent magnet generator. The torque transducer is coupled to the wind turbine transmission shaft which is located by an upper and lower bearing arrangement. The transducer is fixed to the shaft using a steel coupling located by six grub screws. Each of these grub screws has been pre torqued to 20Nm and hence locates on the shaft with zero slip.. On the opposite end of the transducer a spur type driving gear is mounted to drive the generator. This is again located on the transducer shaft using two M10 bolts pre torqued to 20 Nm. The test setup of the turbine is shown below:

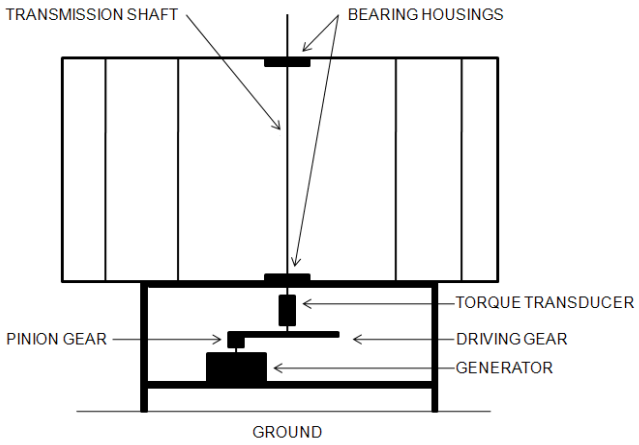

FIGURE 4. Wind turbine transmission/generator configuration

For this set of experiments the generator is used as a brake to control the speed of the rotor. It is this braking effect that loads up the transmission shaft resulting in a torsional moment. The generator has an in built rectifier and allows DC current output to be taken. This DC current is connected in series to a dummy load in the form of a variac resistor bank. A power analyzer is then taken in series between the generator and the load to give realtime data on current, voltage and power. Note for this set of experiments the electrical power output has not been studied.

To characterize the performance of the turbine both torque and speed data is taken from the transducer unit mounted on the shaft. The tranducer gives a 0-5 V output for both torque and speed. The calibration of the transducer has been carried out by the manufacturer and states that 5V = 100Nm of torque. To chracterize the transducer speed output an in house calibration test has been carried out using a large DC servo motor which maintains constant speed.

2.3 Experimental Performance Data

The transducer has two outputs, one for torque and one for speed. Each channel is connected to a data acquisition card which is used to sample the data over a given time period. The data acquisition card is a Sinocera 24 Bit /96 KHz over 4 channelas.

For the purpose of this validation, six different rotor speeds have been studied where the free-stream velocity along with the torque and speed output of the turbine have been sampled. Each data set has been sampled at 750Hz which is shown to give reliable data over a period of 15 seconds. The rotor speed is set using the variac dummy load resistor bank and once set maintains steady state. The following results show the torque output of the turbine as a function of rotor Tip Speed Ratio for a free-stream velocity of 14.8 m/s.

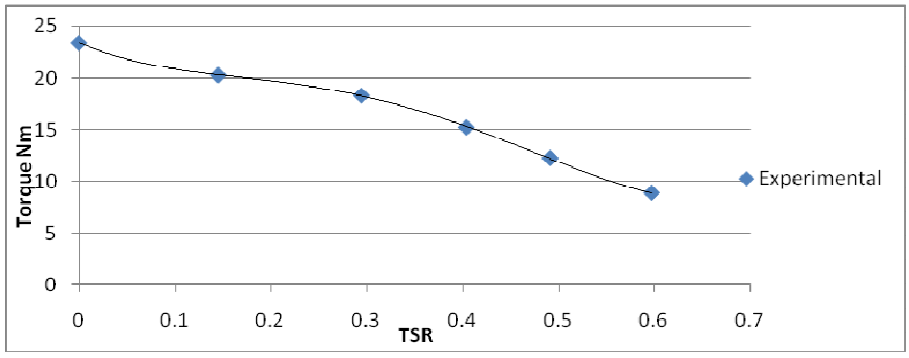

FIGURE 5. Wind turbine torque curve plotted with Tip Speed Ratio

The data obtained here will be used for validating the CFD model for the same conditions. The following section describes the CFD model design.

3. COMPUTATIONAL METHODOLOGY

The CFD software Fluent numerically simulates a virtual flow domain for a given application. It iteratively solves the time-averaged Navier-Stokes equations along with the continuity and auxiliary equations using a control volume approach **[8]**.

The following will describe the design and development of a three-dimensional CFD model that will be used for analysis. The model consists of a rectangular flow domain that is used to represent the physical surroundings of the laboratory area where the experimental testing was carried out. Within this domain is the wind turbine geometry which in this case is represented in full scale at 2.0m diameter x 1.0m in height.

A Multi Reference Frame (MRF) solving technique has been used to perform steady state simulations for different free-stream velocities and rotational speeds. This approach is often known as 'Frozen Rotor' as the rotor geometry is kept stationary. In this case two separate fluid continuums have been created around the stator and rotor blades. The fluid continuum corresponding to the rotor zone is rotated relative to both the stationary rotor blades and the stationary stator fluid zone. It is this rotation of fluid against the stationary blades that is used to compute the forces acting on the rotor and hence the reaction given from the rotor to the fluid.

This is accomplished in the CFD code by incorporating additional acceleration terms which occur due to the transformation from the stationary to the moving reference frame. The flow around the rotor could then be modeled by solving the transport equations in a steady-state manner. The boundary conditions for the rotor fluid are generated by averaging the interface condition between the rotor and the stator.

The flow domain was discretised into a structured grid using hexagonal elements. The region within the turbine was meshed using an unstructured tetrahedral type grid. To ensure high accuracy within the area of interest a high mesh density was used within the turbine zones compared to the outer domain. The ratio of mesh nodal position between the outer domain and turbine zone is limited to 5.

The location of the wind turbine geometry relative to the flow domain boundaries is depicted in figures 6 and 7. Here the turbine is viewed in both the XY and ZX plane as per the axis shown on figure 6. The flow domain used in this study is broken down into a number of discrete volumes which correspond to different zones within the domain. These zones are present to facilitate mesh control in and around the turbine geometry with the aim of improving overall mesh quality.

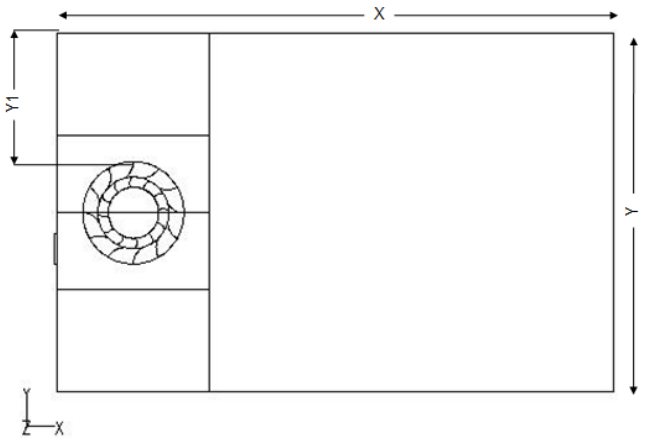

FIGURE 6. Flow domain XY view

Where, X = 11m, Y = 7m, Y1 = 2.5m

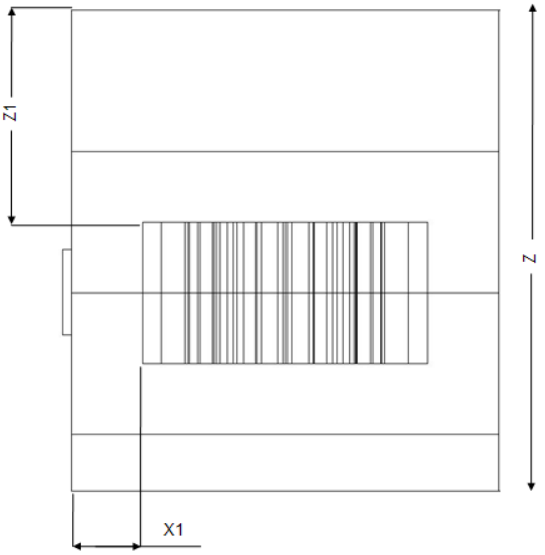

FIGURE 7. Flow domain ZX view

Where, Z = 3.4m Z1= 1.5m X1= 0.5m

3.1 Wind Turbine Geometry

Placed at the origin of the flow domain at X,Y,Z = 0 is the central axis of the turbine located on its bottom face. The turbine used in this study is full scale and hence is 2.0m in diameter and 1.0m in height. The turbine region is made up of three distinct zones as shown in figure 8;

1. The outer stator which consists of 12 equally spaced stationary guide blades.
2. The inner rotor which consists of 12 equally spaced blades which rotate about the Z axis.
3. The volume in the central region of the turbine which is also referred to as the inner core.

Where, r1 = 0.5m, r3 = 0.7m and r4 = 1.0m

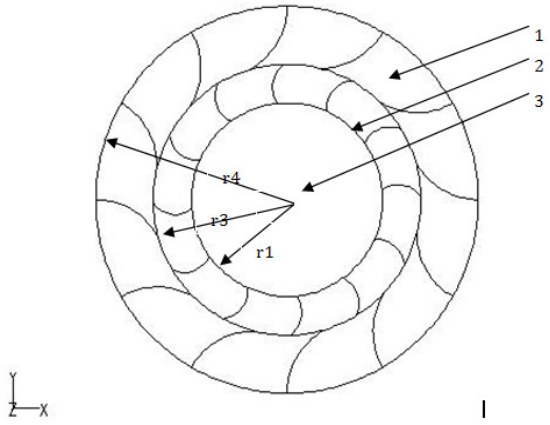

FIGURE 8. Turbine geometry

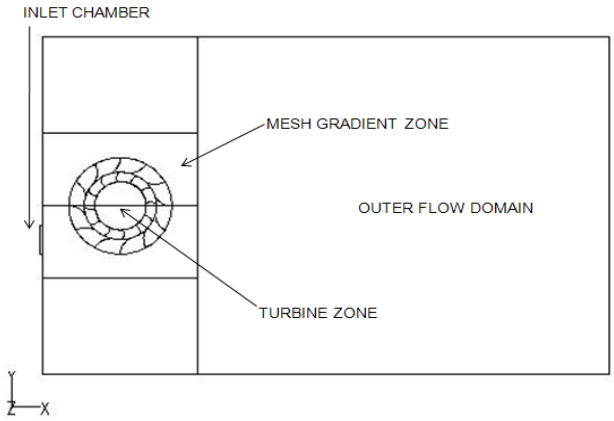

FIGURE 9. Flow domain zones

Surrounding the turbine geometry are small volumes which are used to control the mesh. The distance between the outer radius of the turbine and the faces associated to the control volumes is 0.5m. These regions are split into smaller discrete volumes where their associated lower topoligical entities are used to govern mesh nodal spacing in and around the turbine blades. Due to the high concentration of mesh elements within this region such volumes also reduce computational demands by distributing the mesh evenly over a larger number of volumes. This process signigficantly reduces the memory demands during the meshing process by allowing the mesh to be stored before meshing the next zone.

Beyond these zones exist two further control volumes which make up the remaining fluid domain in the Y direction. These regions are simple singular rectangular volumes which carry the outer flow domain mesh scheme. The size of these volumes is again governed by the dimensions of the laboratory area. The final volume that makes up the flow domain is the outer flow domain. This is again a simple one piece rectangular volume that spans the remaing void in the X direction. These regions and the entire flow domain correspond to the exact dimensions of the laboratory where the baseline set of experimental data was taken. This flow domain and its associated zones are depicted in figure 9.

Within each of these regions exists a number of geometrical enitities ranging from edges, faces and the final volume. Each face within the flow domain has its own individual boundary condition to replicate the physical condition seen in the laboratory. The turbine geometry used here is identical to that used in experiments in terms of length and profile. To reduce computational demands the CFD turbine geometry is simplified to have zero thickness walls compared to the 1.2mm sheet aluminium used on the prototype machine. Such simplifications have been used by other authors in which zero thickness blades are employed in a Rushton turbine **[9]**. This simplification allows for a much higher quality mesh in the blade passage regions by eliminating such a short edge. To validate this effect a preliminary study has been carred out on a two-dimensional model. This model when scaled to three-dimensions showed 2% varaition in torque output between a model with blade thickness and a model without.

3.2 Wind Turbine Boundary Conditions

The stator and rotor fluid rings contain twelve blades each with an associated wall boundary coniditon as shown in figures 10 and 11. These blades are used to govern the fluid volume between them which are referred to as the blade passages. Each turbine blade has two associated geometrical faces which are meshed on both sides. The primary face is defined as blade whereas the secondary surface is defined as blade-shadow.

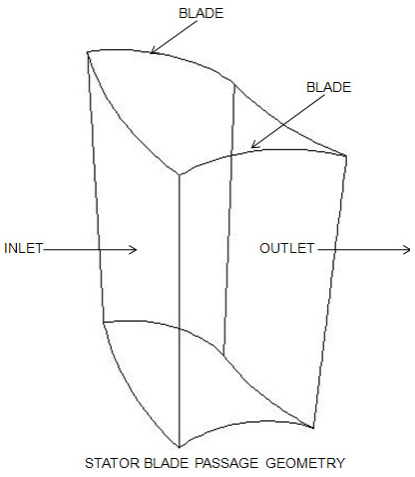

FIGURE 10. Stator blade passage

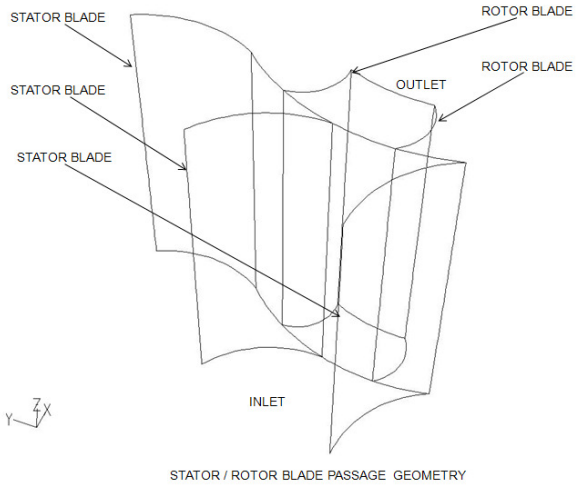

FIGURE 11. Rotor Blade Passage

Each of these faces has been modelled as a non-porous surface using the 'wall' boundary condition within Fluent. It is the forces due to pressure and viscosity on each of these blade walls that will be used to determie the torque output of the rotor. The upper and lower faces within each of the blade passages is defined as a wall boundary to replicate the annular rings that are used on the prototype. The remaining two faces denoted as inlet and outlet on the figure are used as the inlet and outlet to each blade passage cavity. These faces have an interior boundary condition associated with them to allow the fluid to enter and exit without any interaction.

An overview of the turbine zone boundary conditions is provided in figure 12 which shows the velocity inlet boundary with respect to the turbine. Figure 13 depicts the wind turbine geometry in a three-dimensional view where each fluid zone can be seen. Beyond the stator/rotor fluid rings is the central core volume within the domain. This cylindrical volume is the the region at the centre of the turbine and has a diamter of 1.0m and a height of 1.0m. The outer diamter of this volume corresponds to the rotor blade outlet tip radius and is again defined as a fluid continuum.

The boundary conditions used for the remaining flow domain consist of a velocity inlet, pressure outlet and various interior zones. The velocity inlet used in this model replicates that used in the experiment and hence has the same dimensions as the lab test chamber. The orientation of the velocity inlet with respect to the turbine geometry is also the same.

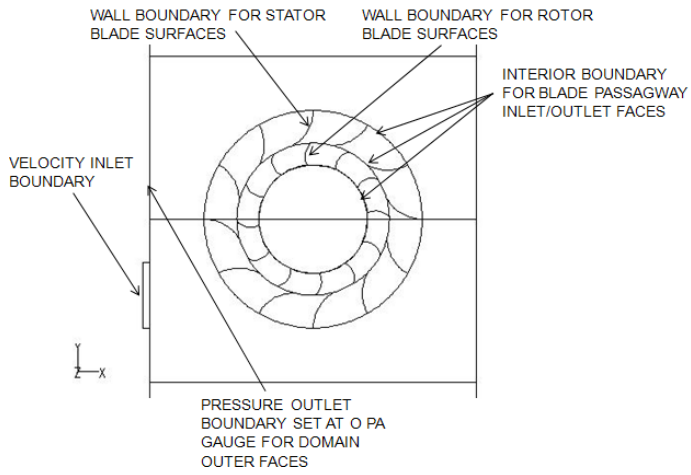

FIGURE 12. Turbine zone boundary conditions

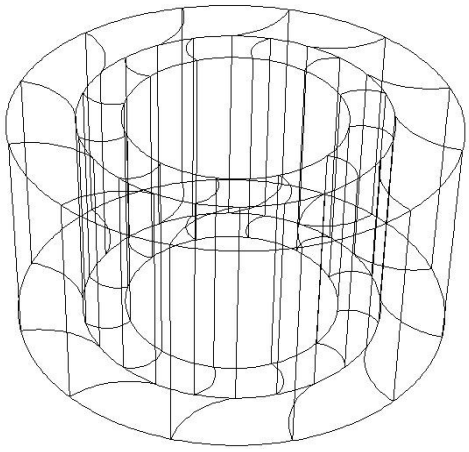

FIGURE 13. Turbine geometry

4. RESULTS

In the following the data obtained from CFD simulations will be presented. Here a series of tests have been carried out to determine the operational characteristics of the machine. The validity of this data is examined by carrying out a comparitive analysis between both experimental and CFD data sets. To ensure a fair comparison the operating conditions used in CFD reflect those present during experiment namely free-stream velocity and rotor speed. The velocity field at the exit of test chamber has been imported into CFD solver Fluent and is taken as the velocity inlet profile. This profile is depcited by figure 14 and shows the velocity inlet boundary in the flow domain in the ZY plane.

4.1 Flow Field Analysis

The flow field around the wind turbine is shown in figure 15 where contours of velocity magnitude depict the non-uniformity in flow. From this figure the jet flow exiting the wind tunnel is captured at a mid plane position within the test chamber which is 0.3m from the cell floor. This flow field is generated under dynamic conditions and for the purpose of this analysis at a Tip Speed Ratio of 0.43.

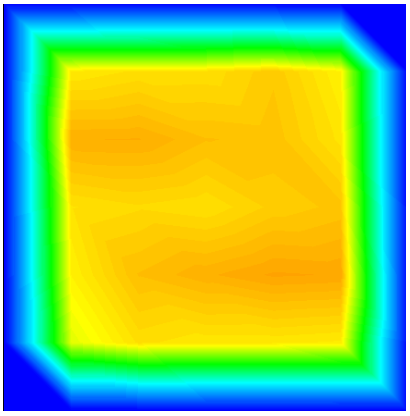

FIGURE 14. Velocity inlet boundary ZY plane

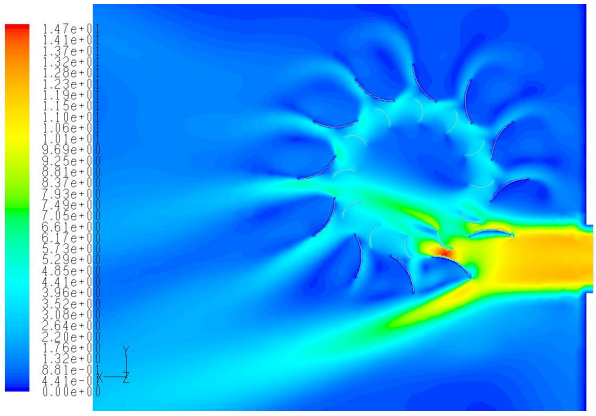

FIGURE 15. Contours of velocity magnitude

The concentration of flow within the stator and rotor passage closest to the exit of the test chamber is shown in detail. This rotor/stator blade passage generates the majority of the turbines torque due to its position relative to the free-stream flow. Further contributions are made to overall turbine torque from the adjacent passage in the anti-clockwise direction which experiences some free-stream flow at similar magnitudes as the primary passage. The adjacent passage in the clockwise direction is shielded by the tip of the stator blade and hence torque generation is restricted.

4.2 Computational Performance Data

The performance characteristics of the wind turbine have been computed using this constant free-stream velocity. The pressure and shear forces acting on the rotor blade surfaces are used to compute the moment acting about the axis of rotation which is taken to be a dimensional torque. Here the performance output of the turbine is investigated under transient conditions by varying the rotational speed of the rotor. The rotor speeds used in this analysis are identicial to those obtained from experiments. Due to the MRF solving technique used it is only possible to compute torque at one rotor blade position. The blade position used in this study corresponds closely to overall mean turbine torque which has been computed during preliminary studies from a series of blade positions. The torque curve of the wind turbine is shown in figure 16.

It can be seen from the figure that the torque output of the rotor is maximum when the rotor is static. Under dynamic conditions an increase in rotor speed results in a decrease in torque in a linear manner. Maximum and minimum torques generated are 23.5 Nm and 6.64 Nm respectively. A comparison is made between between experimental torque data and the data obtained from simulation. Both torque curves are plotted together and show a systematic variation in CFD torque at high rotational speeds.

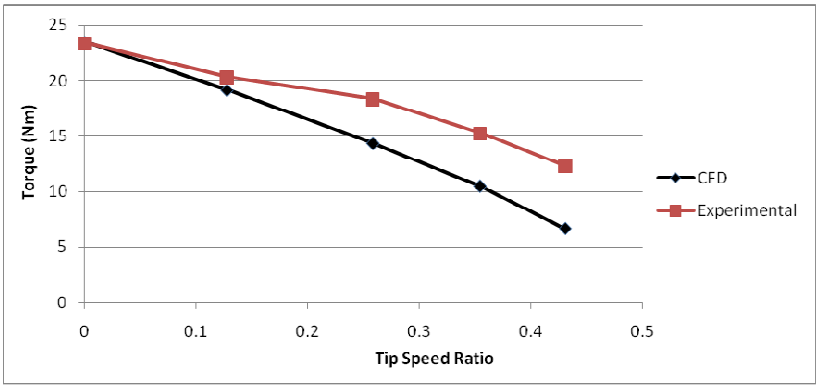

FIGURE 16. CFD wind turbine torque curve plotted with Tip Speed Ratio

It is clear that the experimental torque curve does not follow a linear trend as compared to that obtained from CFD. Upon analysing the curves it is apparant that some additional force is acting on the rotor during experiments or the MRF solving technique used in CFD is not capturing the flow phenomena in sufficient detail. The operating condition at which maximum variation occurs is at a Tip Speed Ratio of 0.43. Here, a percentage variation between experimental and CFD data is in the order of 85% where CFD underpredicts torque.

To determine the reason for such large variation in rotor torque between experimental and CFD data a quanititve investigation has been carried out. It is predicted that both the jet flow and stator blade passage flow characteristics are not being accurately modelled by the CFD code. Using a 4-hole cobra type pressure probe a series of experimental velocity measurements have been taken. These measurements have been taken close to the test chamber wall on the negative Y side due to the nature of flow in this region. These tests are described in the following section.

4.3 Computational Flow Field Validation

To determine the validity of the flow fields predicted by the CFD code, a series of test are carried out experimentally. The region of interrogation is shown in figure 17. This figure shows the wind turbine relative to the exit of the test section in the XY plane. Also shown on this figure is the side wall which has the coordinate Y = 0. For the purpose of the description the view can be assumed to be at the mid-plane of the test section in the Z direction.

The first set of readings are taken at Y = 0 inline with the side wall of the test section. Here a cobra pressure probe faces the flow and is alligned with the side wall using a 3-axis robotic traverse accurate to 0.1mm. This experiment maps the stream-wise flow profile in the +ve X direction as per the figure. The probes starting position is taken to be at X = 280mm which corresponds to 280mm away from the test chamber exit face. Here, three profiles are taken at different heights in the Z direction. The heights are 50mm, 300mm and 600mm all relative to the floor section in the test chamber (Z=0mm).

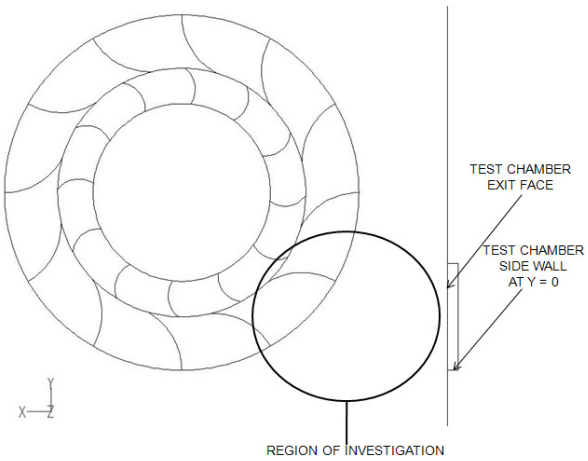

FIGURE 17. Wind turbine interrogation area

The velocity magntiude presented in these figures is dimensionless with respect to the free-stream flow for that set of readings. The stream-wise distance X is also dimensionless with respect to the diameter of the turbine (2.0m). For each height both experimental and CFD data is plotted at a Tip Speed Ratio of 0.43. as per the following figures;

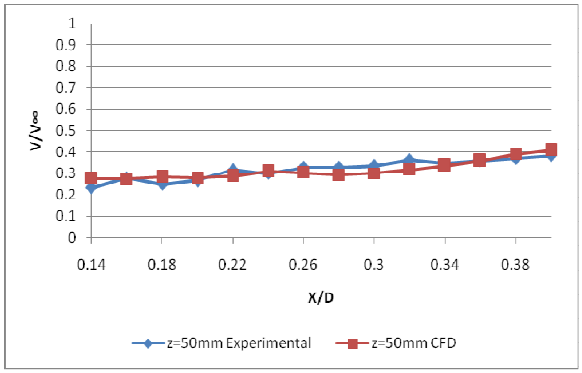

FIGURE 18. Velocity at y=0/z=50mm

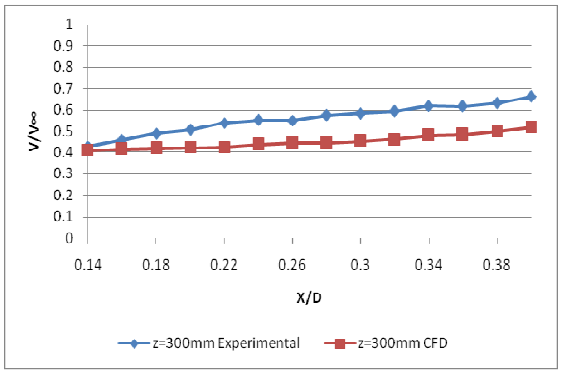

FIGURE 19. Velocity at y=0/z=300mm

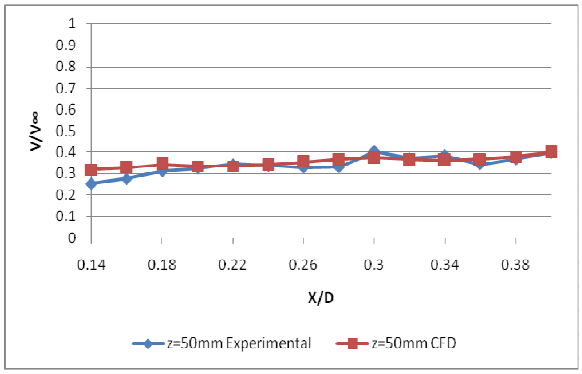

FIGURE 20. Velocity at y=0/z=600mm

It is seen that the stream-wise flow velocity computed from CFD shows similar trends to that obtained from experiments for heights of Z=50mm and Z=600mm. Furthermore, the magnitudes of velocity across this range are of a similar order which gives confidence in the grid used for this simulation.

The data presented for a height of Z=300mm shows a large variation between experimental data and CFD data over the same range. This could be due to the jet effect that brings in additional mass that CFD does not capture.

Given the location of this velocity profile such deviation could be the cause of variations seen in torque output. Due to the systematic nature of turbine torque output variation the effect of rotor speed on a stream-wise flow profile has been computed. This flow profile corresponds to the centre line of the test chamber at Z=300mm and Y=300mm and again a probe is traversed in the X direction towards the turbine.

The range of streamwise traverse varies when compared to the previous figures with 0 - 770mm being used. As per the previous plots both velocity magnitude and stream-wise distance are non-dimensionalised in the same way. The following plots show the effect of rotor speed on streamwise velocity for both experimental and CFD data;

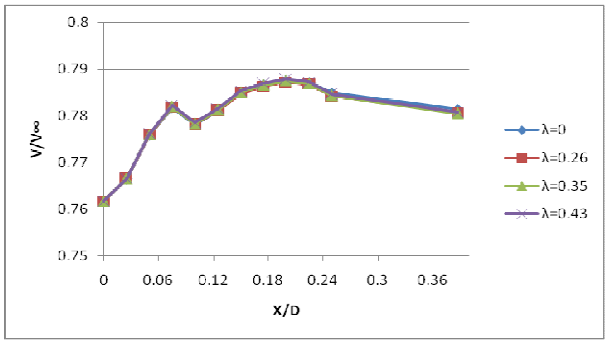

FIGURE 21. CFD velocity at y=300mm/z=300mm

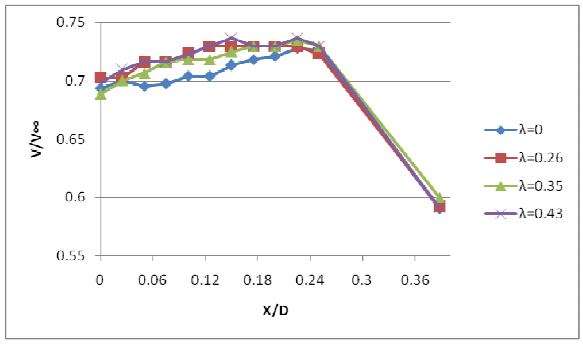

FIGURE 22. Exp velocity at y=300mm/z=300mm

Upon analysing the computational data it is apparant that the stream-wise velocity profile is not affected by rotor speed. This highlights one of the major limitations of the MRF solving technique in that the flow field outside of the rotor fluid region is not affected by the flow phenomena occuring within. Such weak interaction effects occuring in the radial direction are potentially one of the reasons for large variations between experimental and CFD torque output. The experimental streamwise profile as shown in figure 22 shows the effect of rotor speed on the upstream flow profile. The magnitudes of velocity are lowest at a $\lambda = 0$ which is when the rotor is held stationary. As rotor speed increases the upstream velocity increases which indicates some form of suction effect that CFD does not capture. At X/D=0.15 the effect of rotor speed is clear with maximum velocity generated at maximum rotor speed. This suction effect could be the primary factor behind torque variation and its systematic nature.

5. CONCLUSIONS

To summarise, a series of tests have been carried out to determine the performance charactersitics of a novel multi-blade vertical axis wind turbine. Such tests have been undertaken through experimental and computational analysis in which the wind turbine has been subjected to identical conditions. Upon analyizing the torque output of the machine there is a systematic underprediction of torque at high rotor speeds from CFD. The following conclusions have been drawn;

- CFD and its associated MRF solving techniqe underpredict torque systematically at high rotor speeds with 84% percentage variation between CFD and experimental data at λ=0.43.

- It is shown that upon analyzing the local flow field experimentally and compuationally there is further variation in the local velocity field in the stream-wise direction.

- Maximum variation in stream-wise velocity profile occurs at Y=0 and Z=300mm in which a systematic decrease in velocity occurs with an increase in X/D.

- The effect of rotor speed on the local velocity field at the centre line of the test section again in the stream-wise direction has been computed. It is seen that rotor speed has negligible effect on CFD upstream velocity field due to weak interaction effects taken from MRF solving code.

- Experimental velocity field shows opposite trend in that an increase in rotor speed causes local modification to nearby velocity profile. It is shown that an increase in rotor speed results in an increase in velocity due to suction phenomena.

- Based on the latter further work is required to understand interaction effects between rotor under dyanmic conditions and surrounding flow field.

Given the variation in wind turbine performance over a diverse range of operating conditions, future work should be focussed on the development of a micro controller with a view to tracking peak power for a given operational condition.

NOMENCLATURE

$V\infty$ = Free-stream velocity (m/s)

V= Local velocity (m/s)

ω = Angular Velocity (rad/s)

λ = Tip Speed Ratio = $\omega . r/v$

r = Rotor radius (m)

D = Turbine Diameter (m)

REFERENCES

Walker, J. 2009. Wind Power – a firm foundation for a century of renewable energy growth. IOP Conference Series: Earth and Env Science, 6.

BWEA. 2009. England's Regional Renewable Energy Targets: Progress report.

EWEC, 2009. Wind energy review.

EREC, 2007. Renewable energy framework directive.

M.Takao. 2009. A straight bladed vertical axis wind turbine with a directed guide vane row. Thermal Science Vol.18, No.1, 54-57.

Park, S. Lee, T. Sabourin and K. Park. 2009. A novel Vertical Axis Wind Turbine for Distributed & Utility Deployment. Ontario Sustainable Energy Association.

S. Lee, W. Song, J. Park and Y.Kim. 2009. Experimental study on control performance of jet wheel turbo wind turbine. Int Conference on Fluid Machinery.

A.Gosman. 1999. Developments in CFD for industrial and environmental application in wind engineering. J.Wind Eng. Ind. Aerodyn. 81, 21-39.

Zadghaffari, R. Moghaddas, J,S. Revstedt, J. 2008. Large-eddy simulation of turbulent flow in a stirred tank driven by a Rushton turbine. Computers & Fluids. Volume 39. Issue 7